NIH Public Access
Author Manuscript
J Drug Target. Author manuscript; available in PMC 2014 June 03.

Published in final edited form as:
J Drug Target. 2013 December ; 21(10): 956–967. doi:10.3109/1061186X.2013.837470.

Toxicity and efficacy evaluation of multiple targeted polymalic acid conjugates for triple-negative breast cancer treatment

Julia Y. Ljubimova[1,2,3,4], **Jose Portilla-Arias**[#1], **Rameshwar Patil**[#1], **Hui Ding**[#1], **Satoshi Inoue**[1], **Janet L. Markman**[1], **Arthur Rekechenetskiy**[1], **Bindu Konda**[1], **Pallavi R. Gangalum**[1], **Alexandra Chesnokova**[1], **Alexander V. Ljubimov**[2,3,4,5], **Keith L. Black**[1,3,4], and **Eggehard Holler**[1,3,4]

[1]Department of Neurosurgery, Cedars-Sinai Medical Center, Los Angeles, CA, USA

[2]Department of Biomedical Sciences, Cedars-Sinai Medical Center, Los Angeles, CA, USA

[3]Samuel Oschin Comprehensive Cancer Center, Cedars-Sinai Medical Center, Los Angeles, CA, USA

[4]Arrogene, Inc., Santa Monica, CA, USA

[5]Regenerative Medicine Institute, Cedars-Sinai Medical Center, Los Angeles, CA, USA

[#] These authors contributed equally to this work.

Abstract

Engineered nanoparticles are widely used for delivery of drugs but frequently lack proof of safety for cancer patient's treatment. All-in-one covalent nanodrugs of the third generation have been synthesized based on a poly(β-$_L$-malic acid) (PMLA) platform, targeting human triple-negative breast cancer (TNBC). They significantly inhibited tumor growth in nude mice by blocking synthesis of epidermal growth factor receptor, and α4 and β1 chains of laminin-411, the tumor vascular wall protein and angiogenesis marker. PMLA and nanodrug biocompatibility and toxicity at low and high dosages were evaluated *in vitro* and *in vivo*. The dual-action nanodrug and single-action precursor nanoconjugates were assessed under *in vitro* conditions and *in vivo* with multiple treatment regimens (6 and 12 treatments). The monitoring of TNBC treatment *in vivo* with different drugs included blood hematologic and immunologic analysis after multiple intravenous administrations. The present study demonstrates that the dual-action nanoconju-gate is highly effective in preclinical TNBC treatment without side effects, supported by hematologic and immunologic assays data. PMLA-based nanodrugs of the Polycefin™ family passed multiple toxicity and efficacy tests *in vitro* and *in vivo* on preclinical level and may prove to be optimized and efficacious for the treatment of cancer patients in the future.

© 2013 Informa UK Ltd.

Address for correspondence: Julia Y. Ljubimova, MD, PhD, Professor of Neurosurgery and Biomedical Sciences, Director of Nanomedicine Research Center, Department of Neurosurgery, Director of Nanomedicine Program, Samuel Oschin Comprehensive Cancer Center, Cedars-Sinai Medical Center, 8700 Beverly Blvd, AHSPA8307, Los Angeles, CA 90048, USA. Tel: +1-310-423-0834. ljubimovaj@cshs.org.

Declaration of interest
The work was supported by National Institutes of Health grants to Dr J.Y. Ljubimova (R01 CA123495, U01 CA151815 and R01 CA136841) and a grant to Drs E. Holler and J.Y. Ljubimova from Arrogene, Inc., Tarzana, CA, USA.

NIH-PA Author Manuscript
NIH-PA Author Manuscript
NIH-PA Author Manuscript

NIH-PA Author Manuscript

NIH-PA Author Manuscript

NIH-PA Author Manuscript

Keywords

Hematologic; immunogenicity; *in vivo* treatment; nanoconjugate drugs; polymalic acid; toxicity; triple-negative breast cancer

Background

Nanobiopolymers offer a great potential for cancer therapy [1]. Nanodrugs of the first generation relying on passive tumor targeting have already evolved into the third generation delivery systems designed for highly efficient targeting of molecular tumor markers [2] and/or tumor-associated stimuli such as hyperthermia, pH, or tumor-secreted proteinases. While targeting successfully reduces side effects on healthy tissue, toxicity depending on properties of drug carriers and their metabolic products remain a major problem especially during prolonged systemic treatment. For *de novo* engineered nanomaterial, the number of toxic determinants can be very high [3,4]. With this in mind, new nanodrugs were designed with natural-derived building blocks of proven biocompatibility including absence of toxicity, maximal biodegradability, and optimized half-lives sufficient to achieve high drug efficacy at low immunogenicity. We designed an all-in-one covalent drug delivery system termed “Polycefin™”, which carries prodrugs and functional groups chemically bound to polymalic acid (PMLA) as the delivery platform. This biopolymer is superior in chemistry of drug manufacturing, drug loading capacity and structure-based absence of immunogenicity when compared with the biopolymers poly(L-aspartic acid) and poly(L-glutamic acid). The immunogenic and toxic properties of biopolymers and their monomeric units have to be carefully assessed, especially when considering repeated treatments [5]. For example, glutamate produced by enzymatic cleavage of polyglutamic acid can induce apoptosis in neuronal cells and may contribute to glaucoma [6–9], as well as to lysosomal storage disease [10,11]. Poly(γ-D-glutamate) is a toxic component of *Bacillus anthracis* capsule and induces IgG antibodies [12]. Biodegradable micro- and nano-mesoporous silicate particles have been considered as potential drug delivery systems; however, a number of tissues were negatively affected by the treatment. Although local tissue reaction to mesoporous silicates was benign, they caused severe systemic toxicity, such as lung thrombosis and liver cell damage, and entire clearance time of the particles was estimated to be over 4 weeks [13,14].

Polycefin™ nanodrugs have previously demonstrated excellent *in vitro* and *in vivo* tumor targeting and anti-tumor effects [15]. In this report, we have characterized preclinical toxicity and efficacy of novel Polycefin™ variants (Figure 1) designed for the treatment of human triple-negative breast cancer (TNBC) in a xenogeneic mouse model. A variety of assays to assess toxic and immunogenic properties of PMLA platform, single-action nanoconjugates, and complete dual-action nanodrug have been performed. Successful cancer treatment regimens frequently involve repeated drug administration; to this end, we have performed independent experiments for 6 and 12 drug administrations to treat TNBC mouse models for a period of several weeks and evaluated the drugs for multiple toxicity parameters as well as for the effect on tumor size.

NIH-PA Author Manuscript

NIH-PA Author Manuscript

NIH-PA Author Manuscript

Antitumor moieties of these nanodrugs include antisense oligonucleotides (AONs) against epidermal growth factor receptor (EGFR), and/or tumor vascular basement membrane component laminin-411 α4 and β1 chains. EGFR is a member of the EGFR/ErbB/HER family of type-I transmembrane tyrosine kinase receptors [16] and is highly expressed in TNBC. Laminin-411 (subunit composition α4b1γ1) is over-expressed in basement membranes of a variety of aggressive tumors including gliomas and invasive breast cancer [17–19]. Laminin-411 plays an important role in angiogenesis and cell migration [20]. Overexpression of EGFR strongly correlates with poor prognosis, poor response to treatment, and progression of the disease [16]. Anti-EGFR therapy alone or in combination with other drugs has been increasingly recognized as an important treatment strategy for cancer patients [16,21,22]. Several approaches to block EGFR expression and/or function have been effective, including anti-EGFR monoclonal antibodies (mAbs) and EGFR-specific tyrosine kinase inhibitors [23,24]. However, these agents lack tumor specificity causing both acute and chronic side effects [25].

We have previously used PMLA-conjugated anti-TfR antibodies (mAbs) [26,27] for efficient tumor targeting of nanodrugs, and a similar approach was adopted here using a new combination of anti-mouse (MsTfRmAb) and anti-human (HuTfRmAb) TfR mAbs both bound to the polymer platform to treat TNBC. MsTfRmAb functions in transcytosis of the nanoconjugate through the tumor vascular endothelium, and HuTfRmAb targets implanted human breast cancer cells.

The designed nanodrugs also contain polyethylene glycol (PEG), and multiple groups of leucine ethyl ester (LOEt) or trileucine (LLL) (Figure 1). A number of agents that are covalently attached to PMLA, such as morpholino AONs, have entered clinical trials [28,29], and PEG-containing nanoparticles have already been brought to clinic. Although none of the Polycefin™ nanodrug moieties are expected to be toxic, it is known that some biopolymer-based drugs could be toxic and immunogenic [30], necessitating a detailed evaluation of the whole nanodrug for toxicity and immunogenicity *in vitro* and *in vivo* after multiple therapeutic treatments.

Materials and methods

Animal care

All animal experiments were performed in accordance with the protocols approved by the Cedars-Sinai Medical Center, Institutional Animal Care and Use Committee (IACUC). *In vitro* biocompatibility assays were carried out by the Nanotechnology Characterization Laboratory (NCL), National Cancer Institute-Frederick. The rabbit pyrogenic test for endotoxin detection was performed by a GLP-certified laboratory WuXi AppTec, Inc. (St. Paul, MN).

Reagents

Rat anti-mouse TfR mAb R17217 (MsTfRmAb) was from SouthernBiotech (Birmingham, AL). Mouse anti-human TfR mAb RVS10 (HuTfRmAb) was from Millipore Corporation (Billerica, MA), mPEG and C2-maleimide Alexa Fluor 680 from Life Technologies

NIH-PA Author Manuscript

NIH-PA Author Manuscript

NIH-PA Author Manuscript

(Carlsbad, CA), cysteamine (2-mercaptoethyl-1-amine hydrochloride), *N*-hydroxysuccinimide, and all other chemicals of highest available purity were from Sigma-Aldrich (St. Louis, MO). Morpholino-3-NH2 antisense oligonucleotides AON_{EGFR} specific for EGFR mRNA, and AONs specific for laminin-411 α4 and β1 chains mRNAs were custom made by Gene Tools, LLC (Philomath, OR):

AON_{EGFR}: 5′-TCGCTCCGGCTCTCCCGATCAATAC-3′

$AON_{\alpha4}$: 5′-AGCTCAAAGCCATTTCTCCGCTGAC-3′

$AON_{\beta1}$: 5′-CTAGCAACTGGAGAAGCCCCATGCC-3′

Synthesis of PMLA nanoconjugates

The nanoconjugates carry five to seven key components (Figure 1): PMLA as the platform; morpholino AONs inhibiting either EGFR, laminin α4, or laminin β1 protein synthesis; multiple residues of LOEt or LLL functioning as endosomolytic escape unit for the release of nanoconjugates into cell cytoplasm, and $mPEG_{5000}$ increasing the lifetime of the nanoconjugate in the bloodstream. MsTfRmAb targets mouse endothelial cells in tumor vessels, and HuTfRmAb enables drug binding to human tumor cells and mediates nanodrug internalization. Free AONs are released in the cytoplasm by reductive cleavage of the nanodrug disulfide linker. Nanoconjugates and precursors (Figure 1) were synthesized as described [31] involving chemical activation of PMLA pendant carboxyl groups, substitution by amide formation yielding the preconjugate containing 40% LOEt or LLL, 5% $mPEG_{5000}$, and 10% of cysteamine (2-MEA) (% refers to the fraction of carboxyl groups occupied by each particular ligand compared with the carboxyl content of free PMLA). To complete the nanodrug synthesis, activated antibodies and activated AONs were attached. Antibodies were activated by disulfide reduction with tris(2-carboxyethyl)phosphine hydrochloride (TCEP) and coupling to MAL-PEG_{3400}-MAL. Antibody-*S*-Mal-PEG_{3400}-Mal was conjugated at the maleimidyl group with preconjugate-SH. AONs (3′-amine modified) were activated by reacting with *N*-succinimidyl 3-(2-pyridyldithio)propionate (SPDP). The product, PDP-AON, formed disulfide bonds with sulfhydryl groups of the antibody-S-preconjugate yielding the Polycefin-type nanoconjugate. Excess sulfhydryl groups were blocked with pyridyl(dithio)propionate (PDP). The composition of the final nanoconjugate was validated by chemical group analysis of malic acid, AONs, mAbs, $mPEG_{5000}$ in agreement with ±5% of the designed composition. Nanoconjugates were synthesized by the same methods containing either (i) PMLA; (ii) $mPEG_{5000}$ (5%); (iii) PMLA, $mPEG_{5000}$ (5%) and LOEt (40%) or LLL (40%), defined as P; (iv) single-action drug: PMLA, $mPEG_{5000}$ (5%), LOEt (40%) or LLL (40%), AON_{EGFR} (total 2.3%) defined as P/AON_{EGFR} MsTfRHuTfR; (v) single-action drug: PMLA, $mPEG_{5000}$ (5%), LOEt (40%) or LLL (40%), $AON_{\alpha4}$ plus $AON_{\beta1}$ (total 2.3%), MsTfRmAb (0.12%), HuTfRmAb (0.12%) defined as P/$AON_{\alpha4,\beta1}$-MsTfR-HuTfR; (vi) complete dual-action drug: PMLA, $mPEG_{5000}$ (5%), LOEt (40%) or LLL (40%), AON_{EGFR} (2.3%) or $AON_{\alpha4}$ plus $AON_{\beta1}$ (total 2.3%), MsTfRmAb (0.12%), HuTfRmAb (0.12%) defined as P/$AON_{EGFR,\alpha4,\beta1}$-MsTfR-HuTfR. (vii) We have also synthesized a less expensive control nanoconjugate to be used in various *in vitro* assays. It structurally resembles and mimics single-action drugs, except for having anti-TfRmAb replaced by a

NIH-PA Author Manuscript

NIH-PA Author Manuscript

NIH-PA Author Manuscript

non-specific Ms-$IgG_{2a\text{-}k}$ of the same antibody class. This nanodrug is defined as P/AON_{EGFR}-Ms-$IgG_{2a\text{-}k}$. The solutions of nanodrugs and precursors were frozen at –80 ° C where they could be stored in active form for several months. Two cycles of freezing and thawing did not affect mAb integrity and function. The ELISA methods validating functional activity and colocalization on the PMLA platform have been described previously [15].

Production and purification of PMLA

Highly purified, endotoxin-free poly(β-L-malic acid), Mw (weight-averaged) 70 and 100 kDa, polydispersity 1.1, was prepared from the culture broth of *Physarum polycephalum* and purified by DEAE-cellulose chromatography, ethanol precipitation of the calcium salt, size exclusion chromatography, Amberlite-120H^+ conversion into the acid form, and lyophilization forming an amorphous white powder [32]. For i.v. injections, PMLA (50 mg/ml) was neutralized by careful titration with 1 M NaOH, freeze-dried for 72 h and kept for 24 h over phosphorous pentoxide under vacuum at 25 ° C to remove tightly bound water. PMLA Na-salt was NMR pure (<99.9%) and contained Ca <0.2% (Calcium Colorimetric Assay Kit, BioVision Inc., Milpitas, CA), nucleic acid <2 ng/mg (Quant-iT™ dsDNA Broad-Range Assay Kit, Life Technologies, Carlsbad, CA), endotoxin <0.5 EU/mg by Limulus amebocyte lysate (LAL) endpoint assay.

Quantitation of malic acid, mPEG and AON in nanoconjugates

To measure malic acid content in materials of complex composition, HCl at a final concentration of 1 M was added to the sample containing ~1 mM malyl residues in a glass ampoule, sealed tightly and heated for 10 h at 90 ° C. After centrifugation before opening the ampoule, water and HCl were evaporated under reduced pressure, and the residue was dissolved in 50 μl of distilled water. To carry out the malate dehydrogenase assay, 20 μl/well of cleaved samples were distributed into a microwell plate beside standards with malic acid having concentrations of 0.0, 0.2, 0.4, 0.6, 0.8, 1.0, and 1.2 mM. Two-hundred and fifty microliter per well buffer containing 0.6 M glycine, 0.5 M hydrazine, 20 μl NAD (26.7 mg/ml, 40 mM) was added and the mixture incubated at 37 ° C. The dehydrogenase reaction was started by adding 15 μl/well of 0.06 units/ml of malate dehydrogenase from porcine heart (enzyme code EC 1.1.1.37, Sigma-Aldrich, St. Louis, MO). Absorbance at 340 nm was read after 30 min and corrected for background reading. The amount of micromole malic acid per sample was calculated on the basis of the standard curve. For quantitation of mPEG, the amount of complexation with ammonium ferrothiocyanate and extraction with chloroform was obtained by absorbance reading at 510 nm [33]. To quantitate Morpholino AON, the disulfide spacer of the nanopolymer platform was reductively cleaved to release AON by 100 mM dithiothreitol (DTT) at pH 7.4, 1 h at room temperature. Reverse-phase HPLC at 260 nm with free Morpholino AON as standards was carried out for quantitation using reversed phase C18, 5 μm, size 4.6 × 250 mm, gradient: water (0.1% TFA) to acetonitrile (0.1% TFA), flow rate: 1 ml/min. To measure the content of monoclonal IgG antibody, a protein assay kit was used with free mAb as standard (Protein Detector™ ELISA Kit, KPL, Gaithersburg, MD). Percentage (%) of the nanoconjugate loading with Morpholino AON, mAb or $mPEG_{5000}$ was calculated by using the formula % = 100 × (μmol ligand)/(μmol malic acid). Note that the % loading is an average value of variations

NIH-PA Author Manuscript

NIH-PA Author Manuscript

NIH-PA Author Manuscript

referring to polydispersity of the polymer preparation and stochastic nature of conjugation chemistry [34].

Endotoxin measurement and removal

Endotoxin was measured by a quantitative kinetic assay using LAL Pyrogent-5000 kit (Lonza, Walkersville, MD). Individual LAL assays were performed according to the manufacturer's instructions. Sample solutions were prepared in endotoxin-free water. Results were compared with those obtained by dissolving known amounts of USP-certified endotoxin standards in endotoxin-free water. To account for contaminations by inhibitors/enhancers (IEC) affecting LAL activity, test controls (IEC) were prepared by spiking the same amounts of endotoxin standard into the sample solution. Each nanopolymer sample and IEC was tested in duplicate and repeated three times. For each formulation at least four dilutions of the sample were tested. Results were rated acceptable if the standard measured in water and in the sample were the same within 50–200%. The endotoxin sample concentration calculated from different dilutions had to be the same within 25%. These acceptance criteria are in accordance with those mandated by the FDA guideline and USP standard for the LAL test [35].

Removal of endotoxin—Results were obtained with the Triton X-114 extraction method [36]. Briefly, the nanoconjugate, 30 mg, was dissolved in 3 ml phosphate buffer (150 mM, pH 6.8) and the solution was vortexed with 1% Triton X-114 (Sigma-Aldrich, St. Louis, MO) for 5 min. Aliquots of 0.5 ml were transferred into a 1.5-ml conical microcentrifuge tube and placed on ice bath for 5 min to obtain a clear solution. After incubation at 37 ° C for 5 min two phases were formed. After centrifugation at 5000 *g* for 7 s, the upper clear aqueous layer was concentrated by membrane centrifugation. The residual Triton X-114 was removed by gel filtration on an endotoxin-free PD-10 column (GE Healthcare, Piscataway, NJ) pre-washed with LAL reagent water (Lonza, Walkersville, MD). The purified sample was then lyophilized. The amount of endotoxin was measured as above.

Rabbit pyrogenic test

Nanoconjugates were also tested by the Rabbit Pyrogenic USP 151 standard test [35], which indicates toxicity by pyrogens such as bacterial endotoxin. Three New Zealand rabbits were injected via ear vein with 1.5 mg of nanopolymers per kg of body weight. Animal body temperatures were measured before the injection and every 30 min between 1 and 3 h post-injection. An elevation in body temperature of>0.5 ° C above the base temperature is considered positive for pyrogen. The test was carried out by the GLP-certified laboratory WuXi AppTec, Inc. (St. Paul, MN).

Physical characterization of nanobiopolymers

A variety of methodologies were utilized to characterize polymeric nanoconjugates both chemically and physically: size and ζ-potential, HPLC, and ELISA. Sec-HPLC was performed on Hitachi analytical Elite LaChrom HPLC-UV system (Hitachi High Technologies, Pleasanton, CA) and a BioSep-SEC-S 3000 column (Phenomenex, Torrance, CA). Hydrodynamic diameter was measured by dynamic light scattering (DLS) and ζ-potential, by electrophoretic mobility combined with light scattering using Zetasizer Nano

NIH-PA Author Manuscript

NIH-PA Author Manuscript

NIH-PA Author Manuscript

System ZS90 (Malvern Instruments, Malvern, UK), exactly following the conditions described under Assay Cascade Protocols PCC-1 and PCC-2 [37]. Membrane destabilization by nanoconjugates was tested using an artificial liposome system described in previous publications [20,38].

Western blotting of tumor proteins

Subcutaneous tumor tissues from euthanized mice were collected after treatment with PBS, P/AON$_{EGFR}$ MsTfR-HuTfR, P/AON$_{\alpha4,\beta1}$ MsTfR-HuTfR, and P/AON$_{EGFR,\alpha4,\beta1}$-MsTfR-HuTfR. Samples from three tumors in each group were selected at random, homogenized and subjected to western blotting.

Total protein was extracted and concentrations were determined using a BCA assay kit (Bio-Rad Laboratories, Hercules, CA). Extraction buffer contained 2% SDS, 60 mM Tris–HCl pH 6.8, 10% glycerol, with 10% (v/v) protease inhibitor cocktail (AEBSF 104 mM, Aprotinin 80 μM, Bestatin 4 mM, E-64 1.4 mM, Leupeptin 2 mM and Pepstatin A 1.5 mM). Equal amounts of protein (50 μg) were loaded on a 10% SDS–polyacrylamide gel and transferred to nitrocellulose membranes. The membranes were probed with primary antibodies at 1:2000 to phospho-Akt (p-Akt), EGFR (both from Cell Signaling, Boston, MA), laminin α4 chain (clone 8F12; a gift from Dr K. Sekiguchi, Department of Biological Sciences, Osaka University, Osaka, Japan), laminin β1 chain (clone LT3, Abcam, Cambridge, MA), and were normalized to an internal control glyceralde-hyde 3-phosphate dehydrogenase (GAPDH; Cell Signaling, Boston, MA) at 1:5000. Horseradish peroxidase-conjugated secondary antibodies were used for detection followed by enhanced chemiluminescence development (Bio-Rad Laboratories, Hercules, CA).

Cell culture

MDA-MB-468 human TNBC cell line was obtained from American Type Culture Collection (Manassas, VA) and was used as a model to treat TNBC. Cells were cultured in L-15 with 10% FBS and antibiotics.

Treatment of xenogeneic TNBC nude mouse model

Athymic female mice [Tac:Cr:(MCr)-Foxnnm] were purchased from Frederick National Laboratory for Cancer Research, NCI (Frederick, MD). We followed the protocol for tumor inoculation as described in a previous publication [27]. In brief, a total of 1×10^7 EGFR-positive breast cancer MDA-MB-468 cells were suspended in Matrigel (BD Biosciences, Bedford, MA). A 150 μl of cell suspension was injected into the right flanks of mice. The treatments started when tumor sizes reached an average of>120 mm^3 (usually 14 days after injection). Mice were equally distributed into four treatment groups and injected with sterile PBS or P/AON$_{EGFR}$ MsTfR-HuTfR (12.5 mg/kg by AON) or P/AON$_{\alpha4,\beta1}$ MsTfRHuTfR (25 mg/kg by AON) or P/AON$_{EGFR,\alpha4,\beta1}$-MsTfR-HuTfR (37.5 mg/kg by AON) into the tail vein twice a week. Two independent animal studies were conducted with 6 and 12 treatments. Tumor sizes were measured with calipers twice a week, and tumor volumes were calculated using the formula (length × width^2) × (π/6). Two weeks after the last treatment, the animals were anesthetized with 3% isofluraneair mixture and euthanized by cervical dislocation followed by blood retrieval through cardiac puncture for analysis. Tumor

NIH-PA Author Manuscript

NIH-PA Author Manuscript

NIH-PA Author Manuscript

samples were stained with hematoxylin and eosin (H&E) for morphologic examination. There were six to eight animals in each experimental and control group, and the total number of animals was 60.

Nanoconjugate *in vitro* toxicity characterization using human plasma

Various nanoconjugates were assayed at concentrations 0.008, 0.04, 0.2 and 1 mg/ml according to Assay Cascade Protocols [37] at the Frederick National Lab Nanotechnology Characterization Laboratory. The following tests were used: (i) Human hemolysis test (ITA-1), indicator of the potential to cause anemia, jaundice and other pathologic conditions. The colorimetric test measures the amount of hemoglobin released into plasma. (ii) Human platelet aggregation test (ITA-2), quick screening of nanoconjugates for effecting abnormal platelet counts and thus of anticoagulant or thrombogenic properties. (iii) Human Plasma coagulation (ITA-12), incubation with fresh human plasma and assay for delayed coagulation that indicates nanoconjugate-induced depletion of certain coagulation factors. (iv) Total complement activation by western blot analysis (ITA-5.1), a qualitative rapid examination of human plasma after exposure to sample nanoconjugate. Cleavage peptides of C3 complement will be indicated after gel-electrophoresis/blotting by staining with anti-C3 specific antibodies. (v) Enzyme immune assay for quantitative measurement of complement activation (ITA-5.2) after exposure of human plasma to sample nanoconjugate, by capture of complement cleavage products C4b, iC3b, Bb on 96-well plate coated with specific antibodies-peroxidase conjugates. Test includes Doxil® (nanoliposome formulation of Doxorubicin) for comparison with an FDA-approved nanoparticle. (vi) Test for leukocyte proliferation (ITA-6), human lymphocytes are assayed for proliferation, which is stimulated or suppressed by incubation with nanoconjugates using the MTT photometric assay in the absence or presence of phytohemagglutinin (PHA-M). (vii) Nitric oxide production by macrophages (ITA-7), the induction of toxic nitric oxide release from murine macrophage cell line RAW 264.7 in response to nanoconjugate measured using Greiss reagent. (viii) Chemotaxis (ITA-8), the capacity of nanoconjugate to function as chemo-attractant for circulating leukocytes measured in a quantitative model experiment using migration of promyelocytic leukemia cells HL-60 through a filter toward the chemo-attractant. (ix) Phagocytosis assay (ITA-9), where luminol becomes fluorescent when exposed to low pH in phagolysosomes of HL-60 promyelocytic cells, which phagocytize luminol together with nanoparticles. (x) Maturation of dendritic cells (DC) (ITA-14), testing for cytotoxicity by nanoconjugates on DC, or for effects on DC maturation after inflammation stimulated by particular agents, such as LPS.

Effect of PMLA and lead nanoconjugate or precursors on blood cell count, chemical and metabolic panels *in vivo*

PMLA toxicity study—PMLA, Na-salt, as a nanocarrier for toxicity testing was subjected to acute tests by i.v. administration into nude mice. Dosages of 0.1 and 1 g/kg were tested.

To achieve the dosage of 0.1 g/kg in acute tests, 150 μl of solution containing 13.3 mg PMLA/ml, and to achieve 1.0 g/kg, 150 μl of solution containing 133 mg PMLA/ml were injected per 20 g mouse body weight allowing 5 s per injection.

NIH-PA Author Manuscript

NIH-PA Author Manuscript

NIH-PA Author Manuscript

Groups of three mice including the control group were monitored twice every week for weight and neurologic symptoms, respiratory failure, and allergic skin reaction during 14 days. On Day 15, ~1 ml of blood was drawn from mouse's heart by cardiac puncture under the isoflurane anesthesia. CBC, biochemistry and metabolic chemistry panels (serum) were measured at University of California at Los Angeles Division of Laboratory Animal Medicine (DLAM) laboratory (Table 1).

In vivo *study of nanoconjugate toxicity*—Blood samples were collected from the animals that were treated 12 times. This is long-term experiment that started in 14 days after tumor inoculation, performed during 58 days of treatment and tumor size effect was monitored again 14 days after treatment (86 days time-period). The blood was collected for CBC, chemistry and metabolism panels and tested as described in above section.

Statistical analysis

Student's t-test (for two groups) and analysis of variance (ANOVA, for three and more groups) were used to calculate statistical significance of the data. GraphPad Prism4 program (GraphPad Software, San Diego, CA) was utilized. Data are presented as mean ± standard error of mean (SEM). The significance level was set at $p<0.05$.

Results

Preparation of PMLA nanoconjugates

The complete dual-action nanodrug P/AON$_{EGFR,\alpha4,\beta1}$-MsTfR-HuTfR, the single-action nanoconjugates P/AON$_{EGFR}$ MsTfR-HuTfR, and P/AON$_{\alpha4,\beta1}$ MsTfR-HuTfR, and other related nanoconjugates have been synthesized with high chromatographic purity and passed the LAL endotoxin test (<0.5 EU/mg). Hydrodynamic diameters of the lead and the precursor nanoconjugates (numbered 5–8 in Figure 2) followed the signature of other synthesized PMLA-based nanoconjugates, i.e. a typical increase in diameter as a function of molecular weight.

ζ-Potential at neutral pH was lowest for PMLA (–23 mV) and increased to –13.0 mV for PMLA/LOEt (40%), –8.5 mV for the intermediate P, –3.7 mV for P/AON$_{EGFR}$ MsTfR-HuTfR, –5.3 mV for P/AON$_{\alpha4,\beta1}$ MsTfR-HuTfR; and –4.5 mV for P/AON$_{EGFR,\alpha4,\beta1}$-MsTfR-HuTfR, whereas nanoconjugates containing LLL for endosomal release were considerably more negative, i.e. –28 mV for P/LLL (40%). The ζ-potential of the lead nanoconjugate was slightly negative, ideal for attaching to cell membranes and allowing for receptor-mediated internalization [39,40]. The close to neutral ζ-potential of LOEt-containing nanoconjugates could be a source of cytotoxicity. According to the results of the artificial membrane destabilization test, LOEt-containing nanoconjugates could easily cross biologic membranes at neutral pH [20,38,41]. In contrast, LLL-containing nanoconjugates, because of their very negative ζ-potential, were unable to do so at this pH. However, these nanoconjugates could penetrate through endosomal membranes into surrounding cytoplasm at pH<5.5 typically found in late endosomes/lysosomes.

NIH-PA Author Manuscript

NIH-PA Author Manuscript

NIH-PA Author Manuscript

The nanoconjugates inhibit growth of EGFR-positive triple-negative breast tumors in nude mice

We investigated the therapeutic effect of the novel nanobioconjugates by i.v. treatment using the subcutaneous inoculation of human MDA-MB-468 cells overexpressing EGFR. The in vivo experiments included PBS (control), the complete dual-action nanodrug P/$AON_{EGFR,\alpha4,\beta1}$-MsTfR-HuTfR, and the single-action nanoconjugates P/AON_{EGFR} MsTfR-HuTfR and P/$AON_{\alpha4,\beta1}$ MsTfR-HuTfR. Tumor growth inhibition data are based on two independent experiments with six and twelve treatments. The six-treatment regimen with P/$AON_{\alpha4,\beta1}$ MsTfR-HuTfR showed significant tumor inhibition, $p<0.05$ versus PBS group (Figure 3a). The single-action P/AON_{EGFR} MsTfR-HuTfR drug and especially the dual-action drug P/$AON_{EGFR,\alpha4,\beta1}$-MsTfR-HuTfR, showed increased tumor growth inhibition ($p<0.001$ versus PBS group).

In the twelve-treatment regimen, the nanoconjugate P/$AON_{\alpha4,\beta1}$ MsTfR-HuTfR had marginal effect, whereas a significant anti-tumor effect was seen again upon treatment with P/AON_{EGFR} MsTfR-HuTfR, and even greater effect, with complete drug P/$AON_{EGFR,\alpha4,\beta1}$-MsTfR-HuTfR (Figure 3a). The data suggest that in this setting, the complete dual-action drug showed synergy with the anti-EGFR single-action drug (Figure 3a). To test at the molecular level for possible synergy between these AON-based nanodrugs, tumors of three mice per group were extracted after the end of 12 treatment-experiment and proteins examined by western blotting (Figure 3b). P/AON_{EGFR} MsTfR-HuTfR reduced the amount of both EGFR and its downstream signaling intermediate pAkt, but had no effect on the expression of laminin α4 and β1 chains. Similarly, treatment with P/$AON_{\alpha4,\beta1}$ MsTfR-HuTfR had no effect on EGFR, but reduced the amounts of laminin α4 chain and pAkt, although the effect on laminin β1 chain was very weak and variable. In contrast, treatment with dual-action nanodrug P/$AON_{EGFR,\alpha4,\beta1}$- MsTfR-HuTfR significantly inhibited the expression of EGFR, pAkt, laminin β1 chain and to a slightly lesser extent, laminin α4 chain, consistent with cross-talk between EGFR and the laminins through laminin-binding integrin receptors [42,43]. Thus, in both 6 and 12 treatment regimens the dual-action nanoconjugate with three AONs demonstrated significant efficacy in inhibiting TNBC growth and angio-genesis. The treatment regimen for six i.v. administrations of complete drug may be largely enough for TNBC growth inhibition. In the future, for possible human cancer treatment, the regimen of six-time i.v. administrations might be multiplied to obtain the best anti-cancer effect.

PMLA nanoplatform evaluation *in vivo*

Low and high dosage of PMLA does not affect blood cell count, metabolic and chemistry panels. To study the toxicity of PMLA as the nanoconjugate platform *in vivo*, we examined its effects on nude mice using two concentrations 0.1 g/kg (low) and 1.0 g/kg (high). The results for blood cell count, metabolic and chemistry panels are shown in Table 1. Neither loss in body weight (data not shown), nor any abnormalities in blood cell counts or biochemical parameters were observed.

NIH-PA Author Manuscript

NIH-PA Author Manuscript

NIH-PA Author Manuscript

Twelve-treatment regimen (chronic exposure) of nude mice by nanoconjugates does not induce toxic changes in blood cell count, metabolic and chemistry panels

During 12 treatments, i.e. i.v. injections every 3 days of nanoconjugates P/AON$_{EGFR,\alpha4,\beta1}$-MsTfR-HuTfR, P/AON$_{\alpha4,\beta1}$ MsTfR-HuTfR, or P/AON$_{EGFR}$ MsTfR-HuTfR, nude mice did not exhibit adverse physical effects such as body weight loss (data not shown), morbidity, or death indicating that all treatments were well tolerated. Gross- and micro-histopathology of all major organs/tissues by H&E staining did not reveal any visible morphologic changes (data not shown). Complete blood count (CBC) cell counts, metabolic and chemistry panels (Table 2) demonstrate normal parameters in all blood tests for all the injected nanoconjugates compared with untreated group of mice and the control (PBS) group. These results suggest that the tested nanoconjugates were non-toxic, and that the complete P/AON$_{EGFR,\alpha4,\beta1}$-MsTfR-HuTfR nanodrug qualified as safe and effective agent for the treatment of TNBC.

PMLA nanoplatform and nanoconjugate toxicity testing *in vitro*

Most of the *in vitro* results presented here refer to Assay Cascade Protocols [37] and were obtained by the Nanotechnology Characterization Laboratory (NCL). These protocols were developed for further nanodrug testing according to FDA guidelines.

Absence of pyrogenic (endotoxin) and hematologic toxicity of PMLA and nanoconjugates—*In vivo* rabbit pyrogenic test: The result for the complete nanoconjugate P/AON$_{EGFR,\alpha4,\beta1}$-MsTfR-HuTfR was an increase in body temperature of <0.5 ° C in each of three rabbits indicating the absence of pyrogenic material in agreement with the absence of endotoxin in preparations measured by LAL test (<0.5 EU). All the results presented below are obtained with endotoxin-free PMLA and drugs.

Hematologic toxicity of PMLA and nanoconjugates: Hemolysis (ITA-1) assay confirmed that for all nanoconju-gates and PMLA hemolysis was below the detection limit at concentrations from 0.008 to 1.0 mg/ml (not shown here). Platelet aggregation (ITA-2): PMLA did not induce significant aggregation of human platelets (i.e. <20% of positive control; data not shown). P/AON$_{EGFR}$-Ms-IgG$_{2a\text{-}k}$, a mimic of single-action drugs with the same amount of AON and antibody (Figure 4), and similar nanoconjugates tended to inhibit collagen-induced platelet aggregation. Plasma coagulation (ITA-12): At concentration of 0.04 mg/ml and above, PMLA prolonged coagulation time in the thrombin time assay (Figure 5). Prolongation was referred to inhibition of the coagulation pathway possibly due to the binding of PMLA to coagulation factor XII. Binding was likely due to the presence of negative charges on PMLA as is shown for other compounds like heparin [44]. In the activated partial thromboplastin time assay, similar prolongation was seen at PMLA concentrations of 0.2 mg/ml and higher. At the same time, no increase in prothrombin time was seen at any PMLA concentration up to 1 mg/ml (Figure 5). Importantly, no interference with plasma coagulation parameters was observed for P/AON$_{EGFR}$-Ms-IgG$_{2a\text{-}k}$ in the thrombin, activated partial thromboplastin, and prothrombin-time assays (Figure 6).

NIH-PA Author Manuscript

NIH-PA Author Manuscript

NIH-PA Author Manuscript

Immune response tests—These tests were conducted to examine possible adverse effects of PMLA and mimic nanoconjugate on the functions of immune cells as indicators of immunotoxicity [37].

Complement activation (ITA-5.1 and ITA-5.2): PMLA at 1 mg/ml showed virtually no complement activation assessed by the appearance of C3 split product on western blots (Figure 7, top). The simplified nanodrug version P/AON$_{EGFR}$-Ms-IgG$_{2a\text{-}k}$ showed low levels (<5% with regard to positive control) of complement activation revealed by western blotting for human, mini pig, rat, mouse, and Cynomolgus monkey (Figure 7, middle). In the quantitative enzyme immunoassay, complement activation (forming iC3b) by P/AON$_{EGFR}$-Ms-IgG$_{2a\text{-}k}$ was weakly elevated at the highest concentration of 1 mg/ml corresponding to only 20% of the level measured for FDA-approved Doxil® (Figure 7, bottom). Leukocyte proliferation (ITA-6): PMLA (Figure 8, top) and mimic nanoconjugate (not shown) did not induce proliferation of human leukocytes. The data indicate that the nanoconju-gates were not immunostimulatory toward unprimed human leukocytes. Nitric oxide production by macrophages (ITA-7): PMLA (Figure 8, middle) and mimic nanoconjugate (not shown) tested at 0.008–1.0 mg/ml did not induce oxidative burst indicated by the absence of nitric oxide secretion (no inflammation-related response). Chemotaxis (ITA-8): Only insignificant induction of macrophage chemotaxis (not shown here) was observed for PMLA and mimic nanoconjugate (0.008–1.0 mg/ml). Phagocytosis (ITA-9): PMLA (Figure 8, bottom) and mimic nanoconjugate (up to 1.0 mg/ml) were not internalized by phagocytosis and had no significant effect on phagocytosis of zymosan (data not shown). Both these assays thus did not show any adverse effects on macrophage functions. Maturation of DC (ITA-14): PMLA (0.008– 1.0 mg/ml) did not induce maturation of monocyte-derived DC and had no effect on LPS-induced maturation. PMLA did not induce maturation markers CD80, CD83, CD86, and did not affect CD14 expression (data not shown). Therefore, no effect on DC was observed as well.

Discussion

Nanodrug delivery systems have received increasing attention because such multifunctional systems can provide powerful and fairly specific multi-modal treatments of cancer. Other than its antitumor treatment efficacy, the multifunctionality of the polymer molecule together with its biodegradability bear great hopes for future anti-cancer applications. Polycefin™ nanoconjugates are examples of the third generation of tumor-targeted nanodrugs and have been successfully used to treat tumors in animal models of primary brain and breast cancer [5,20,26,27,45].

In contrast to non-conjugated delivery vehicles such as nanoparticles, micelles, and liposomes that are prone to uncontrolled leaking of (toxic) cargo due to spontaneous or environmental effects, nanodrugs of the Polycefin™ family are designed as fully covalently conjugated delivery system [5]. Polycefins have high drug loading capacity, easy synthetic accessibility and biodegradability. Yet, for potential clinical applications, it is crucial to understand that the polymer is biocompatible and non-toxic.

NIH-PA Author Manuscript

NIH-PA Author Manuscript

NIH-PA Author Manuscript

The high anticancer efficacy of various nanoconjugates in the treatment of TNBC mouse models was demonstrated here. The primary target was EGFR that is known as cancer cell growth stimulator and angiogenic factor acting through its downstream signaling including the Akt pathway, which plays an important role in breast cancer cell growth and migration [46]. Overexpression of EGFR in TNBC strongly correlates with poor patient prognosis [47]. In the present study, nanoconjugates were designed for treatment of EGFR-expressing breast cancer and tested for efficacy in repetitive treatments. The complete dual-action nanodrug on the PMLA nanoplatform with covalently attached AONs targeting EGFR and angiogenic laminin-411, combined with TfR mAbs for extravasation and targeted tumor uptake, was readily synthesized and administrated systemically. AON as anti-cancer drugs have been successfully used to treat experimental tumors [48,49]. In particular, Morpholino AONs used in our work are stable in circulation and are being increasingly used in gene therapy [50,51]. TNBC treatment efficacy was very high in case of the nanodrug with AON_{EGFR} that also contained laminin-targeting $AON_{\alpha 4}$ and $AON_{\beta 1}$ (Figure 3). Western blotting confirmed synergistic effect of three AONs not observed when nanoconjugates contained either AON_{EGFR} or $AON_{\alpha 4}$ plus $AON_{\beta 1}$ were used indicating the importance of cross-talk between EGFR and laminin-411 containing α4 and β1 chains.

We also present ample evidence that the PMLA nanoplat-form was well tolerated *in vivo* and *in vitro* in extreme dosages without toxicity and immune reactions. PMLA and the nanoconjugates purified free of endotoxin activated neither complement nor macrophages. They also did not show appreciable toxicity for cultured liver HepG2 and kidney LLC-PK1 human cells even at *in vitro* dosages as high as 1 mg/ml (data not shown here).

Analysis of blood biochemistry, metabolic assays, CBC panel, and immunotoxicity did not reveal any abnormalities compatible with toxicity *in vitro* or *in vivo* even after 12 repeated systemic nanodrug injections. In particular, hemolysis was not observed, and only minimum complement activation was noticed at very high dosage of nanoconjugates (1.0 mg/kg), which is 37 times higher than nanodrug therapeutic concentration. The degree of activation was far less than that observed with FDA-approved Doxil. The nanoconjugates did not induce significant platelet aggregation, and did not affect coagulation pathways. Special tests excluded the presence of pyrogenic material in the nanoconjugate preparations.

Under conditions of advanced cancer, continuous treatment could be necessary until the tumor regresses [27,52,53]. In clinic, however, in many cases the chemotherapy must be discontinued due to life threatening side effects such as liver, kidney, cardio- or neurotoxicity. The significant side effects, in particular thrombocytopenia and leukopenia, induction of thrombosis and suppression of immune system (immunotoxi-city) are the major indications for treatment interruption. This situation with prolonged treatment was tested by conducting 12 consecutive nanodrug systemic administrations against growing TNBC over the period of 8 weeks. As a result, the tumor growth was significantly inhibited, and the treatment was well tolerated without noticeable abnormalities in blood cell counts, multiple biochemistry parameters, and with no immunostimulatory or immunosuppressive response.

In conclusion, the present study demonstrates that the used nanoconjugates are highly effective in preclinical TNBC treatment without side effects, supported by extensive

NIH-PA Author Manuscript

NIH-PA Author Manuscript

NIH-PA Author Manuscript

hematologic and immunologic data. Including our previously published data, Polycefin™ nanodrugs passed multiple tests *in vitro* and *in vivo* for antitumor efficacy and toxicity, and may be potentially used as optimal drug delivery systems for cancer treatment.

Acknowledgments

The authors are grateful to the members of our subcontractor, Nanotechnology Characterization Laboratory (NCL, National Cancer Institute-Frederick, Frederick, MD), for performing the analysis of PMLA and different nanopolymers, conducting various *in vitro* immunologic tests with these nanopolymers, and helpful discussions.

References

1. Hudson D, Margaritis A. Biopolymer nanoparticle production for controlled release of biopharmaceuticals. Crit Rev Biotechnol. 2013 [Epub ahead of print]. doi: 10.3109/07388551.2012.743503.
2. Gu FX, Karnik R, Wang AZ, et al. Targeted nanoparticles for cancer therapy. Nano Today. 2007; 2:14–21.
3. Chandna P, Khandare JJ, Ber E, et al. Multifunctional tumor-targeted polymer–peptide–drug delivery system for treatment of primary and metastatic cancers. Pharm Res. 2010; 27:2296–306. [PubMed: 20700631]
4. Sandoval MA, Sloat BR, Lansakara PD, et al. EGFR-targeted stearoyl gemcitabine nanoparticles show enhanced anti-tumor activity. J Control Release. 2012; 157:287–96. [PubMed: 21871505]
5. Ljubimova JY, Fujita M, Ljubimov AV, et al. Poly(malic acid) nanoconjugates containing various antibodies and oligonucleotides for multitargeting drug delivery. Nanomedicine. 2008; 3:247–65. [PubMed: 18373429]
6. Ruiz F, Alvarez G, Ramos M, et al. Cyclosporin A targets involved in protection against glutamate excitotoxicity. Eur J Pharmacol. 2000; 404:29–39. [PubMed: 10980260]
7. Kumar DM, Perez E, Cai ZY, et al. Role of nonfeminizingestrogen analogues in neuroprotection of rat retinal ganglion cells against glutamate-induced cytotoxicity. Free Radic Biol Med. 2005; 38:1152–63. [PubMed: 15808412]
8. Zhang Y, Bhavnani BR. Glutamate-induced apoptosis in neuronal cells is mediated via caspase-dependent and independent mechanisms involving calpain and caspase-3 proteases as well as apoptosis inducing factor (AIF) and this process is inhibited by equine estrogens. BMC Neurosci. 2006; 7:49–71. [PubMed: 16776830]
9. Gupta N, Yücel YH. Glaucoma as a neurodegenerative disease. Curr Opin Ophthalmol. 2007; 18:110–14. [PubMed: 17301611]
10. Kishore BK, Lambricht P, Laurent G, et al. Mechanism of protection afforded by polyaspartic acid against gentamicin-induced phospholipidosis. II. Comparative *in vitro* and *in vivo* studies with poly-l-aspartic, poly-l-glutamic and poly-d-glutamic acids. J Pharmacol Exp Ther. 1990; 255:875–85. [PubMed: 1700819]
11. Kishore BK, Maldague P, Tulkens PM, Courtoy PJ. Poly-d-glutamic acid induces an acute lysosomal thesaurismosis of proximal tubules and a marked proliferation of interstitium in rat kidney. Lab Invest. 1996; 74:1013–23. [PubMed: 8667606]
12. Schneerson R, Kubler-Kielb J, Liu TY, et al. Poly(γ-d-glutamic acid) protein conjugates induce IgG antibodies in mice to the capsule of *Bacillus anthracis*: a potential addition to the anthrax vaccine. Proc Natl Acad Sci USA. 2003; 100:8945–50. [PubMed: 12857944]
13. Hudson SP, Padera PF, Langer R, Kohane DS. The biocompatibility of mesoporous silicates. Biomaterials. 2008; 29:4045–55. [PubMed: 18675454]
14. Liu T, Li L, Teng X, et al. Single and repeated dose toxicity of mesoporous hollow silica nanoparticles in intravenously exposed mice. Biomaterials. 2011; 32:1657–68. [PubMed: 21093905]
15. Fujita M, Lee BS, Khazenzon NM, et al. Brain tumor tandem targeting using a combination of monoclonal antibodies attached to biopoly(β-l-malic acid). J Control Release. 2007; 122:356–63. [PubMed: 17630012]

NIH-PA Author Manuscript

NIH-PA Author Manuscript

NIH-PA Author Manuscript

16. Baselga J. Why the epidermal growth factor receptor? The rationale for cancer therapy. Oncologist. 2002; 7:2–8. [PubMed: 12202782]
17. Ljubimova JY, Fujita M, Khazenzon NM, et al. Association between laminin-8 and glial tumor grade, recurrence, and patient survival. Cancer. 2004; 101:604–12. [PubMed: 15274074]
18. Fujita M, Khazenzon NM, Bose S, et al. Overexpression of β1-chain-containing laminins in capillary basement membranes of human breast cancer and its metastases. Breast Cancer Res. 2005; 7:R411–21. [PubMed: 15987446]
19. Ljubimova JY, Lakhter AJ, Loksh A, et al. Overexpression of a4 chain-containing laminins in human glial tumors identified by gene microarray analysis. Cancer Res. 2001; 61:5601–10. [PubMed: 11454714]
20. Ding H, Inoue S, Ljubimov AV, et al. Inhibition of brain tumor growth by intravenous poly(β-l-malic acid) nanobioconjugate with pH-dependent drug release. Proc Natl Acad Sci USA. 2010; 107:18143–8. [PubMed: 20921419]
21. Pal SK, Childs BH, Pegram M. Triple negative breast cancer: unmet medical needs. Breast Cancer Res Treat. 2011; 125:627–36. [PubMed: 21161370]
22. Esposito CL, Passaro D, Longobardo I, et al. A neutralizing RNA aptamer against EGFR causes selective apoptotic cell death. PLoS One. 2011; 6:e24071. [PubMed: 21915281]
23. Agrawal A, Gutteridge E, Gee JM, et al. Overview of tyrosine kinase inhibitors in clinical breast cancer. Endocr Relat Cancer. 2005; 12:S135–44. [PubMed: 16113090]
24. Huang S, Armstrong EA, Benavente S, et al. Dual-agent molecular targeting of the epidermal growth factor receptor (EGFR): combining anti-EGFR antibody with tyrosine kinase inhibitor. Cancer Res. 2004; 64:5355–62. [PubMed: 15289342]
25. Widakowich C, de Castro G Jr, de Azambuja E, et al. Side effects of approved molecular targeted therapies in solid cancers. Oncologist. 2007; 12:1443–55. [PubMed: 18165622]
26. Inoue S, Ding H, Portilla-Arias J, et al. Polymalic acid-based nanobiopolymer provides efficient systemic breast cancer treatment by inhibiting both HER2/*neu* receptor synthesis and activity. Cancer Res. 2011; 71:1454–64. [PubMed: 21303974]
27. Inoue S, Patil R, Portilla-Arias J, et al. Nanobiopolymer for direct targeting and inhibition of EGFR expression in triple negative breast cancer. PLoS One. 2012; 7:e31070. [PubMed: 22355336]
28. Popplewell L, Koo T, Leclerc X, et al. Gene correction of a Duchenne muscular dystrophy mutation by meganuclease-enhanced exon knock-in. Hum Gene Ther. 2013; 24:692–701. [PubMed: 23790397]
29. Moulton HM. *In vivo* delivery of morpholino oligos by cell-penetrating peptides. Curr Pharm Des. 2013; 19:2963–9. [PubMed: 23140456]
30. Li C. Poly(l-glutamic acid) anticancer drug conjugates. Adv Drug Deliv Rev. 2002; 54:695–713. [PubMed: 12204599]
31. Lee BS, Fujita M, Khazenzon NM, et al. Polycefin, a new prototype of a multifunctional nanoconjugate based on poly(β-l-malic acid) for drug delivery. Bioconjug Chem. 2006; 17:317–26. [PubMed: 16536461]
32. Ljubimova JY, Fujita M, Khazenzon NM, et al. Nanoconjugate based on polymalic acid for tumor targeting. Chem Biol Interact. 2008; 171:195–203. [PubMed: 17376417]
33. Nag A, Mitra G, Ghosh PC. A colorimetric assay for estimation of polyethylene glycol and polyethylene glycolated protein using ammonium ferrothiocyanate. Anal Biochem. 1996; 237:224–31. [PubMed: 8660570]
34. Mullen DG, Desai AM, Waddell JN, et al. The implications of stochastic synthesis for the conjugation of functional groups to nanoparticles. Bioconjug Chem. 2008; 19:1748–52. [PubMed: 18729391]
35. Dobrovolskaia MA, Neun BW, Clogston JD, et al. Ambiguities in applying traditional Limulus amebocyte lysate tests to quantify endotoxin in nanoparticle formulations. Nanomedicine. 2010; 5:555–62. [PubMed: 20528451]
36. Aida Y, Pabst MJ. Removal of endotoxin from protein solutions by phase separation using Triton X-114. J Immunol Methods. 1990; 132:191–5. [PubMed: 2170533]

NIH-PA Author Manuscript

NIH-PA Author Manuscript

NIH-PA Author Manuscript

37. Assay Cascade Protocols, Frederick National Lab. Nanotechnology Characterization Laboratory. Available from: http://ncl.cancer.gov/working_assay-cascade.asp [last accessed 14 Aug 2013]
38. Ding H, Portilla-Arias J, Patil R, et al. Polymalic acid peptide copolymers: design and optimization for endosomolytic drug delivery. Biomaterials. 2011; 32:5269–78. [PubMed: 21514661]
39. Lorenz MR, Holzapfel V, Musyanovych A, et al. Uptake of functionalized, fluorescent-labeled polymeric particles in different cell lines and stem cells. Biomaterials. 2006; 27:2820–8. [PubMed: 16430958]
40. Wilhelm C, Billotey C, Roger J, et al. Intracellular uptake of anionic superparamagnetic nanoparticles as a function of their surface coating. Biomaterials. 2003; 24:1001–11. [PubMed: 12504522]
41. Ding H, Portilla-Arias J, Patil R, et al. Distinct mechanisms of membrane permeation induced by two polymalic acid copolymers. Biomaterials. 2013; 34:217–25. [PubMed: 23063368]
42. Edick MJ, Tesfay L, Lamb LE, et al. Inhibition of integrin-mediated crosstalk with epidermal growth factor receptor/Erk or Src signaling pathways in autophagic prostate epithelial cells induces caspase-independent death. Mol Biol Cell. 2007; 18:2481–90. [PubMed: 17475774]
43. Yu X, Miyamoto S, Mekada E. Integrin a2b1-dependent EGFR receptor activation at cell–cell contact sites. J Cell Sci. 2000; 113:2139–47. [PubMed: 10825287]
44. Elgue G, Sanchez J, Egberg N, et al. Effect of surface-immobilized heparin on the activation of adsorbed factor XII. Artif Organs. 1993; 17:721–6. [PubMed: 8215954]
45. Fujita M, Khazenzon NM, Ljubimov AV, et al. Inhibition of laminin-8 *in vivo* using a novel poly(malic acid)-based carrier reduces glioma angiogenesis. Angiogenesis. 2006; 9:183–91. [PubMed: 17109197]
46. Kallergi G, Agelaki S, Kalykaki A, et al. Phosphorylated EGFR and PI3K/Akt signaling kinases are expressed in circulating tumor cells of breast cancer patients. Breast Cancer Res. 2008; 10:R80. [PubMed: 18822183]
47. Liu D, He J, Yuan Z, et al. EGFR expression correlates with decreased disease-free survival in triple-negative breast cancer: a retrospective analysis based on a tissue microarray. Med Oncol. 2012; 29:401–5. [PubMed: 21264531]
48. Mainelis G, Seshadri S, Garbuzenko OB, et al. Characterization and application of a nose-only exposure chamber for inhalation delivery of liposomal drugs and nucleic acids to mice. J Aerosol Med Pulm Drug Deliv. 2013 [Epub ahead of print] PMID: 23530772.
49. Zhang M, Garbuzenko OB, Reuhl KR, et al. Two-in-one: combined targeted chemo and gene therapy for tumor suppression and prevention of metastases. Nanomedicine. 2012; 7:185–97. [PubMed: 22339132]
50. Hiroi N, Funahashi A, Kitano H. Comparative studies of suppression of malignant cancer cell phenotype by antisense oligo DNA and small interfering RNA. Cancer Gene Ther. 2006; 13:7–12. [PubMed: 16082382]
51. Kinali M, Arechavala-Gomeza V, Feng L, et al. Local restoration of dystrophin expression with the morpholino oligomer AVI-4658 in Duchenne muscular dystrophy: a single-blind, placebo-controlled, dose-escalation, proof-of-concept study. Lancet Neurol. 2009; 8:918–28. [PubMed: 19713152]
52. Craft BS, Hortobagyi GN, Moulder SL. Adjuvant biologic therapy for breast cancer. Cancer J. 2007; 13:156–61. [PubMed: 17620764]
53. Ding H, Helguera G, Rodríguez JA, et al. Polymalic acid nanobioconjugate for simultaneous immunostimulation and inhibition of tumor growth in HER2/*neu*-positive breast cancer. J Control Release. 2013 [Epub ahead of print] PMID: 23770212.

NIH-PA Author Manuscript

NIH-PA Author Manuscript

NIH-PA Author Manuscript

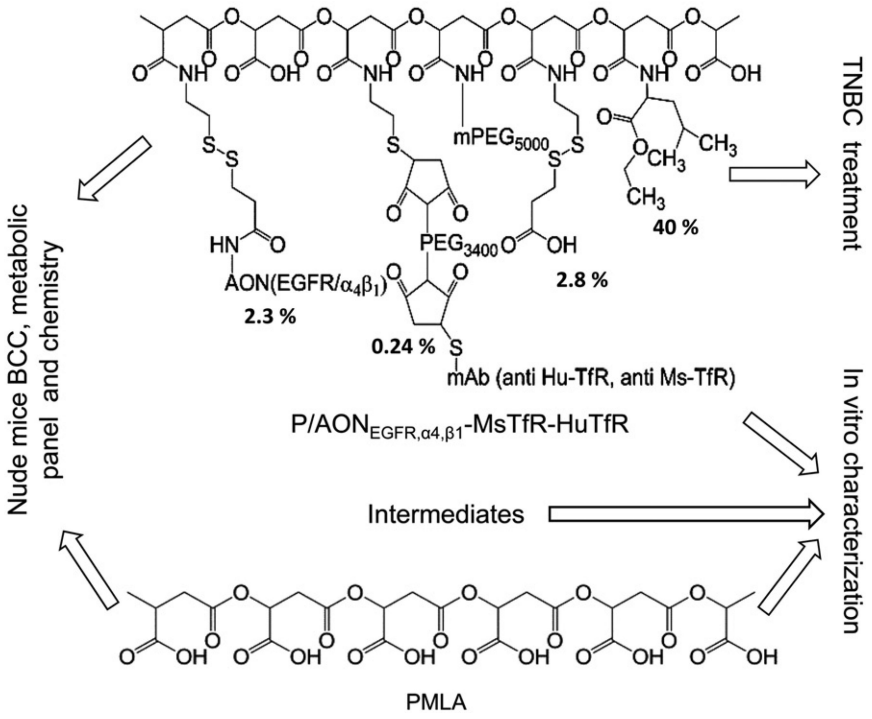

Figure 1.

Composition of nanoconjugates and performed experiments evaluating their anti-tumor efficacy, biocompatibility and toxicity.

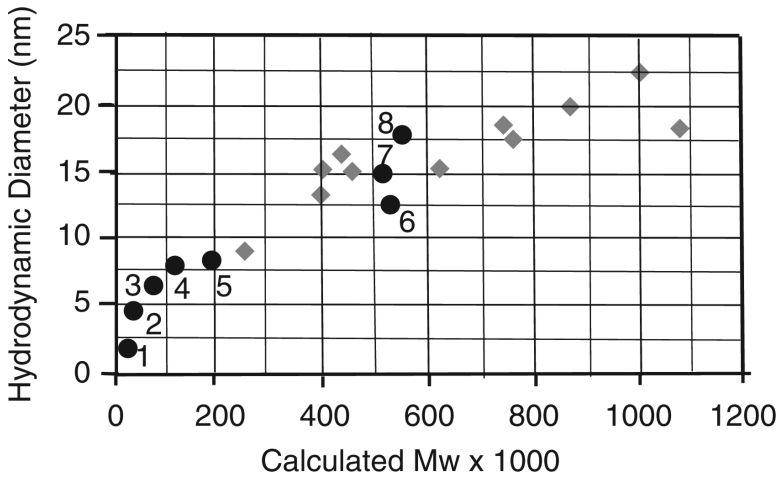

Figure 2.

Hydrodynamic diameters of PMLA nanoconjugates assuming spherical particles are shown as a function of calculated molecular weights. Data points numbered 1–4 (circles) refer to free polymalic acid of different molecular weight, and data points numbered 5–8 (circles) refer to various nanodrugs. All other data points (squares) refer to PMLA-based nanodrugs of different composition regarding antibodies, AONs, endosome escape units (LLL or LOEt), mPEG, and in several cases chemotherapeutics synthesized by us and published before [20,31,42]. Diameters were calculated by the Malvern Zetasizer software (Malvern Instruments, Malvern, UK). Free PMLA and various nanoconjugates with loads of different composition are compared. Molecular weights of PMLA were obtained by sec-HPLC method with polystyrene sulfonate as standards and for nanoconjugates by calculation according to their structures. Indicated numbers refer to: 1–4. PMLA Mw 20 000–100 000; 5. P; 6. P/AON$_{EGFR}$ MsTfR-HuTfR; 7. P/AON$_{\alpha4,\beta1}$ MsTfR-HuTfR; 8. P/AON$_{EGFR\alpha4,\beta1}$ MsTfR-HuTfR.

NIH-PA Author Manuscript NIH-PA Author Manuscript NIH-PA Author Manuscript

NIH-PA Author Manuscript

NIH-PA Author Manuscript

NIH-PA Author Manuscript

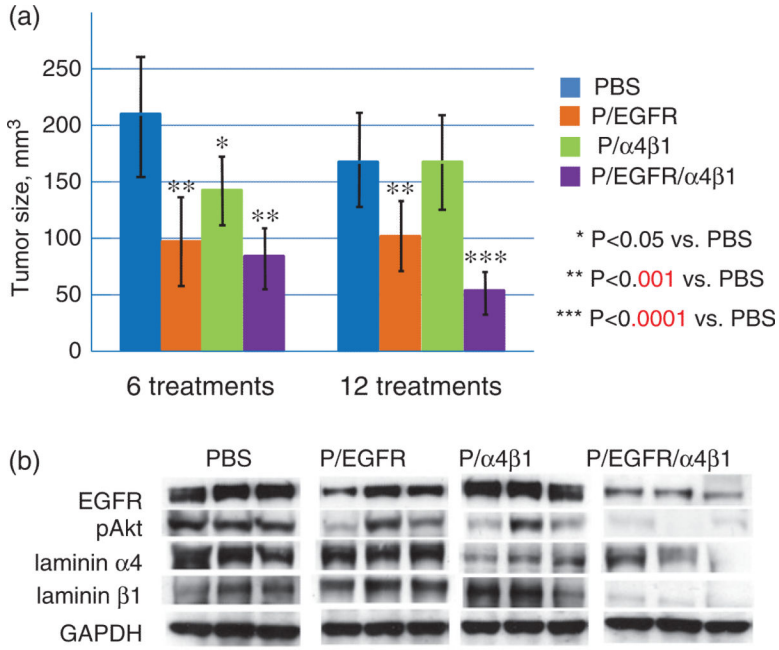

Figure 3.

Treatment of nude mice bearing TNBC. (a) Efficacy showing reduction in tumor size during 6 and 12 treatments. Highest efficacy was obtained with complete dual-action drug when all three AONs were together on the same platform. (b) Western blots of tumor protein extracts upon various treatments showing effects on the expression of EGFR, laminin α4 chain, laminin β1 chain and pAkt. The strongest inhibitory effect is obtained with dual-action nanoconjugate P/AON$_{EGFR,\alpha4,\beta1}$-MsTfR-HuTfR. Results are shown for three mice after 12 treatments with nanoconjugates P/AON$_{EGFR}$ MsTfR-HuTfR (P/EGFR), P/AON$_{\alpha4,\beta1}$ MsTfR-HuTfR (P/α4β1) and P/AON$_{EGFR,\alpha4,\beta1}$-MsTfR-HuTfR (P/EGFR/α4β1).

NIH-PA Author Manuscript

NIH-PA Author Manuscript

NIH-PA Author Manuscript

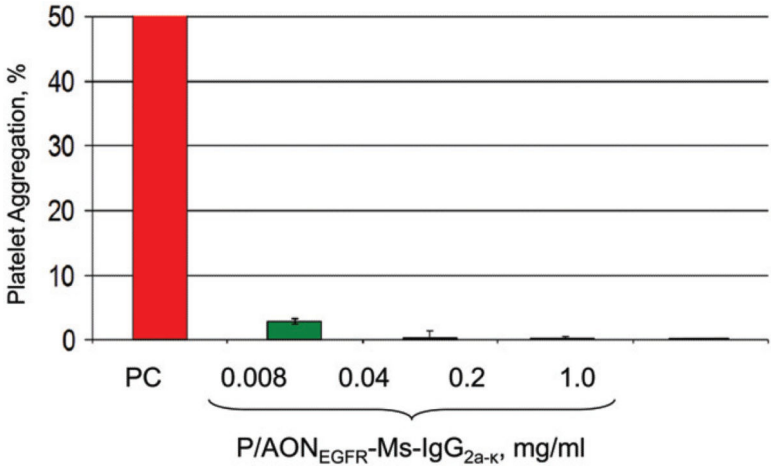

Figure 4.

In vitro testing of platelet aggregation. ITA-2 assay demonstrates the absence of human platelet aggregation for the single-action nanodrug mimic P/AON$_{EGFR}$-Ms-IgG$_{2a-k}$ at different concentrations. PC-positive control.

NIH-PA Author Manuscript

NIH-PA Author Manuscript

NIH-PA Author Manuscript

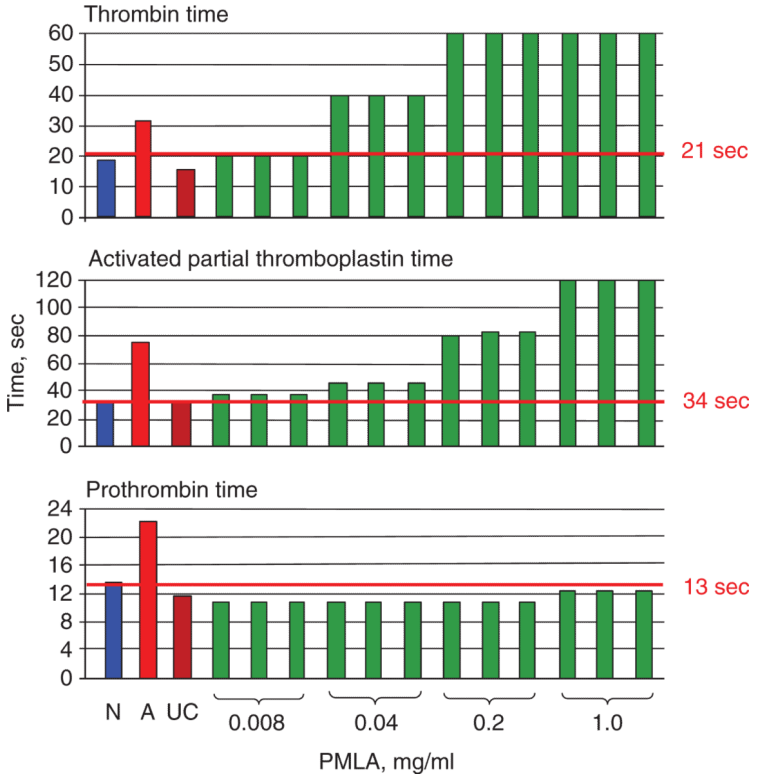

Figure 5.

ITA-2 demonstrates coagulation parameters thrombin time, activated partial thromboplastin time and prothrombin time for nanoplatform PMLA at different concentrations. Three independent samples analyzed in duplicate. PMLA increase thrombin time, activated partial thromboplastin time, but has no effect on prothrombin time. N, normal plasma standard; A, abnormal plasma standard; UC, untreated control. The red line indicates the clinical standard cut-off for normal coagulation time for each of the tests.

NIH-PA Author Manuscript

NIH-PA Author Manuscript

NIH-PA Author Manuscript

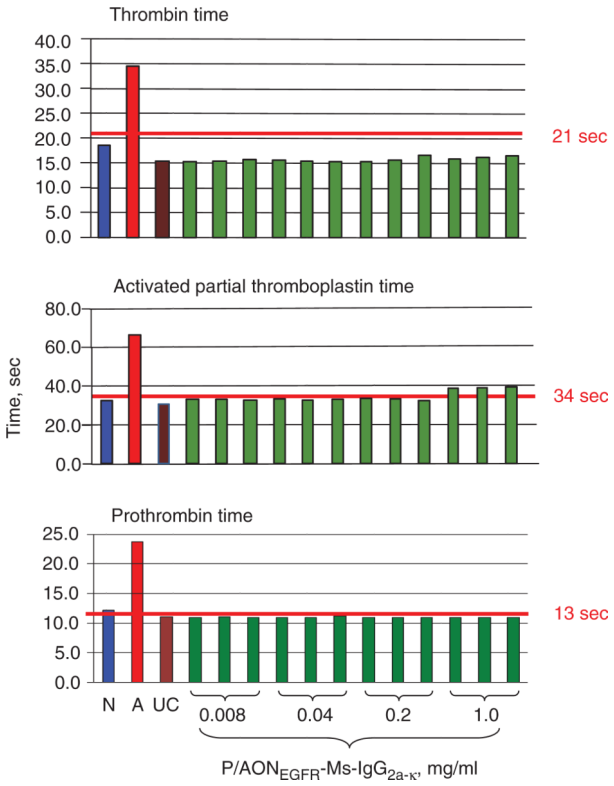

Figure 6.

ITA-2 demonstrates coagulation parameters thrombin time, activated partial thromboplastin time and prothrombin time for P/AON$_{EGFR}$-Ms-IgG$_{2a-k}$ at different concentrations. The nanoconjugate does not change coagulation parameters. Three independent samples analyzed in duplicate. N, A, UC, and the red line as explained on Figure 5.

NIH-PA Author Manuscript

NIH-PA Author Manuscript

NIH-PA Author Manuscript

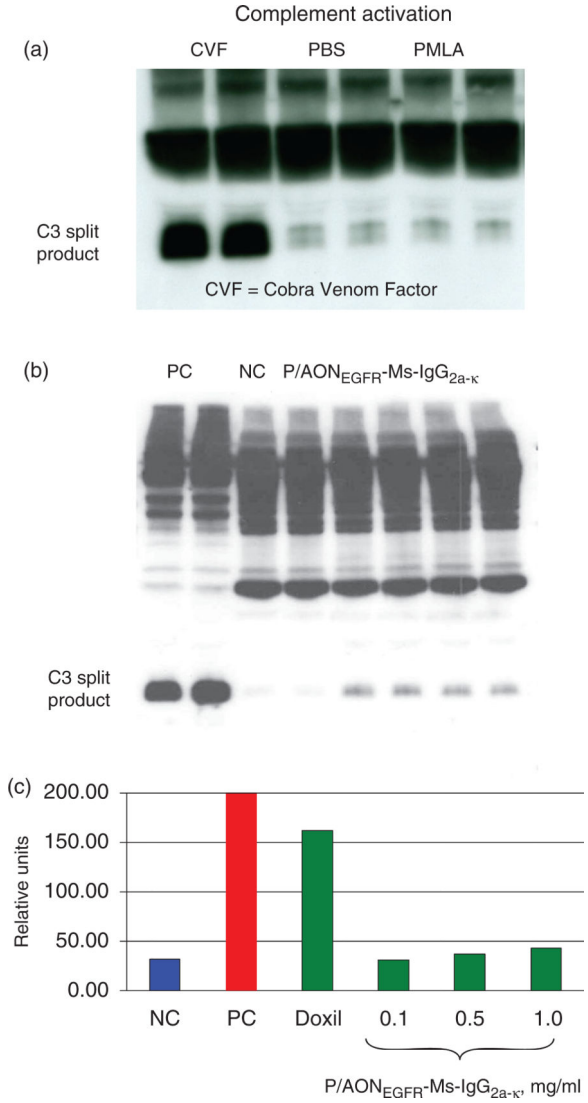

Figure 7.

C3-Complement activation by P/EGFR-like nanoconjugate analyzed by western blotting (a and b) and by enzyme immune assay (c). PMLA was inactive, whereas P/EGFR-like nanoconjugate showed some but low complement activation resulting in hydrolytic cleavage of C3. Doxil (0.67 mg/ml), an FDA-approved nanodrug, was five-times more active than the nanoconjugate. NC, negative control; PC, positive control; CVF, Cobra Venom Factor.

NIH-PA Author Manuscript

NIH-PA Author Manuscript

NIH-PA Author Manuscript

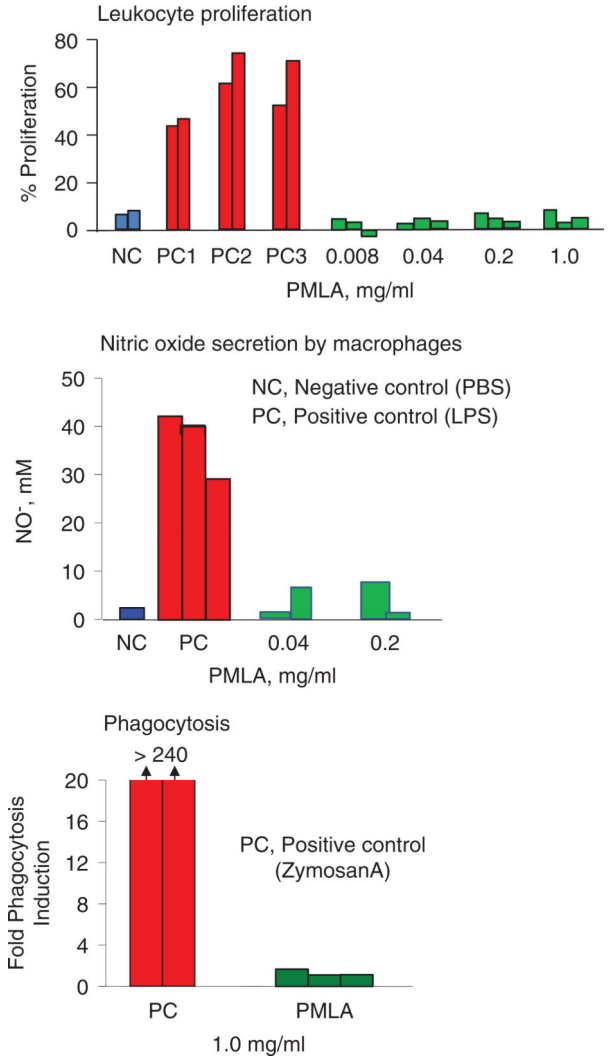

Figure 8.

Testing immunogenicity of PMLA. The nanobiopolymer does not induce leukocyte proliferation, macrophage secretion of NO or phagocytosis. PC1–PC3 sera from three different donors.

NIH-PA Author Manuscript

NIH-PA Author Manuscript

NIH-PA Author Manuscript

Table 1

Complete blood count, chemistry and metabolic panel of nude mice after i.v. injection of 0.1 g/kg PMLA-Na and 1.0 g/kg PMLA-Na.

Test (n = 3)	Normal*	PBS	0.1 g/kg PMLA-Na	1.0 g/kg PMLA-Na
Complete blood count (CBC)†				
WBC (10^3/μl)	0.22–9.78	5.65 ± 0.35	6.51 ± 2.22	8.84 ± 1.79
RBC (10^6/μl)	0.22–9.86	8.90 ± 0.64	9.13 ± 0.60	8.59 ± 0.27
HGB (g/dl)	0.1–15.6	15.1 ± 1.2	15.5 ± 1.2	14.2 ± 0.4
HCT (%)	1.2–59.6	45.3 ± 6.4	44.1 ± 2.5	39.76 ± 1.0
PLT (10^3/μl)	230–2206	854 ± 47	952 ± 26	877 ± 20
Chemistry and metabolic panel‡				
ALT (U/l)	39–188	76 ± 19	65 ± 25	61 ± 29
AST (U/l)	52–421	292 ± 36	168 ± 19	366 ± 35
ALB (g/dl)	2.5–3.8	2.1 ± 0.2	2.3 ± 0.3	1.8 ± 0.3
TBIL (mg/dl)	0.2–0.6	0.6 ± 0.3	0.6 ± 0.2	0.6 ± 0.3
TPR (g/dl)	4.5–7.0	3.5 ± 0.2	3.7 ± 0.3	3.0 ± 0.3
PHOS (mg/dl)	8.1–17.3	11.8 ± 1.8	11.2 ± 0.6	9.8 ± 1.0
Ca (mg/dl)	8.9–11.9	7.3 ± 1.8	7.7 ± 0.6	7.2 ± 1.0
BUN (mg/dl)	9–36	17 ± 2	21 ± 1	20 ± 5
CREA (mg/dl)	0.2–0.5	0.2 ± 0.1	0.2 ± 0.1	0.2 ± 0.0
Na (mmol/l)	129.8–169.9	145.1 ± 0.1	145.2 ± 0.14	145.9 ± 0.12
K (mmol/l)	7.25–11.93	7.84 ± 2.36	7.84 ± 2.45	7.69 ± 2.14
Cl (mmol/l)	98.8–163.0	114.3 ± 0.5	115.1 ± 4.52	117.6 ± 4.32

*Nu/Nu mouse (age 8–10 weeks) clinical pathology data, North American Colonies (January 2008–December 2011), Charles River, Wilmington, MA.

†WBC: white blood cell count, RBC: red blood cell count, HGB: Hemoglobin, HCT: Hematocrit, PLT: Platelet count.

‡ALT: Serum alanine aminotransferase, AST: Aspartate aminotransferase, ALB: Albumin, TBIL: Total bilirubin, TPR: Total protein, PHOS: Phosphorus, Ca: Calcium, BUN: Urea nitrogen, CREA: Creatinine, Na: Sodium, K: Potassium, Cl: Chloride.

NIH-PA Author Manuscript

NIH-PA Author Manuscript

NIH-PA Author Manuscript

Table 2

Complete blood count (CBC), chemistry and metabolic panel of TNBC-bearing nude mice after 12 treatments during 58 days with lead nanoconjugate and precursor nanoconjugates.

Test (n = 3)	Normal*	PBS	P/EGFR	P/α4β1	P/EGFR/α4β1
Complete blood count (CBC)†					
WBC (10^3/μl)	0.22–9.78	6.55 ± 1.70	6.53 ± 2.29	7.59 ± 2.37	6.83 ± 2.60
RBC (10^6/μl)	0.22–9.86	8.73 ± 1.70	6.84 ± 1.69	8.22 ± 0.98	6.84 ± 1.69
HGB (g/dl)	0.1–15.6	12.9 ± 2.7	10.5 ± 3.2	12.4 ± 1.6	12.4 ± 1.2
HCT (%)	1.2–59.6	51.3 ± 10.2	40.6 ± 11.3	47.8 ± 6.5	47.5 ± 4.3
PLT (10^3/μl)	230–2,206	705 ± 49	759 ± 206	789 ± 64	770 ± 54
Chemistry and metabolic panel‡					
ALT (U/l)	39–188	34 ± 8	37 ± 12	38 ± 5	32 ± 2
AST (U/l)	52–421	89 ± 20	88 ± 21	77 ± 11	59 ± 20
ALB (g/dl)	2.5–3.8	2.8 ± 0.1	2.6 ± 0.1	2.9 ± 0.1	2.8 ± 0.2
TBIL (mg/dl)	0.2–0.6	0.2 ± 0.0	0.2 ± 0.1	0.3 ± 0.0	0.3 ± 0.1
TPR (g/dl)	4.5–7.0	4.7 ± 0.4	4.5 ± 0.1	4.8 ± 0.1	4.8 ± 0.2
PHOS (mg/dl)	8.1–17.3	11.5 ± 1.9	11.7 ± 2.0	9.7 ± 2.0	7.9 ± 2.5
Ca (mg/dl)	8.9–11.9	9.5 ± 0.2	9.6 ± 2	9.7 ± 0.1	9.6 ± 0.3
BUN (mg/dl)	9–36	22 ± 2	26 ± 2	22 ± 3	22 ± 4
CREA (mg/dl)	0.2–0.5	0.3 ± 0.0	0.0 ± 0.0	0.3 ± 0.0	0.3 ± 0.0
Na (mmol/l)	129.8–169.9	150.5 ± 1.6	156.6 ± 1.1	151.4 ± 1.1	154.1 ± 0.6
K (mmol/l)	7.25–11.93	3.73 ± 0.26	4.17 ± 0.15	4.19 ± 0.3	3.72 ± 0.2
Cl (mmol/l)	98.8–163.0	114.3 ± 0.8	120.2 ± 0.3	115.1 ± 1.2	117.6 ± 0.8

*Nu/Nu mouse (age 8–10 weeks) clinical pathology data, North American Colonies (January 2008–December 2011), Charles River, Wilmington, MA.

†WBC: White blood cell count, RBC: Red blood cell count, HGB: Hemoglobin, HCT: Hematocrit, PLT: Platelet Count.

‡ALT: Serum alanine aminotransferase, AST: Aspartate aminotransferase, ALB: Albumin, TBIL: Total bilirubin, TPR: Total protein, PHOS: Phosphorus, Ca: Calcium, BUN: Urea nitrogen, CREA: Creatinine, Na: Sodium, K: Potassium, Cl: Chloride.